Xylan Deconstruction by Environmental Bacterium Caulobacter crescentus

Viet Bui[1], Rhoda Inkoom[1], and Gopal Periyannan[1]

[1]Eastern Illinois University

February 14, 2023

Abstract

Bacterial species display unique and common molecular mechanisms for nutrient acquisition depending on their habitat. Molecular details of xylan utilization by plant pathogens and human commensal bacteria have been reported but no significant reports can be found for environmental bacteria. Caulobacter crescentus is a gram-negative, oligotrophic, environmental bacterium with unique adaptations for growth in low-nutrient conditions. C. crescentus' genome codes for a repertoire of genes that can facilitate xylan utilization as a carbon source for growth. Polymeric xylan and xylan-derivative use by C. crescentus was investigated in this work. Growth, enzyme, metabolite, and gene expression analyses show possible membrane-bound enzymes for xylan deconstruction on the cell surface while enzymes for further deconstruction of xylan-derived oligosaccharides are concentrated in the periplasm. TonB-dependent transporter (TBDT) inhibition data suggest that TBDT may be involved in the transport of xylo-oligosaccharides across the outer membrane. Collectively, data suggest xylan binding onto the bacterial surface and deconstruction and the xylan fragment uptake across the outer membrane. A comprehensive model for xylan utilization by C. crescentus develops to show features of previously proposed gut and plant pathogenic bacterial models. This study further advances the molecular level understanding of xylan derived nutrient acquisition in environmental bacteria.

Xylan Deconstruction by Environmental Bacterium *Caulobacter crescentus*

Viet Bui | Rhoda E. Inkoom | Gopal R. Periyannan

Department of Chemistry and Biochemistry, Eastern Illinois University, Charleston, IL 61920

Keywords: Xylan, *Caulobacter crescentus,* degradation, polysaccharide, xylanase

Correspondence

Gopal R. Periyannan

Department of Chemistry and Biochemistry

600 Lincoln Avenue

Charleston, IL 61920

E-mail: grperiyannan@eiu.edu

217 218 9573

Abbreviations:

TBDT: TonB-Dependent Transporters, XOS: Xylo-oligosaccharides, GH: Glycoside hydrolase

Abstract

Bacterial species display unique and common molecular mechanisms for nutrient acquisition depending on their habitat. Molecular details of xylan utilization by plant pathogens and human commensal bacteria have been reported but no significant reports can be found for environmental bacteria. *Caulobacter crescentus* is an environmental, gram-negative, oligotrophic bacterium with unique adaptations for growth in low-nutrient conditions. *C. crescentus'* genome codes for a repertoire of genes that can facilitate xylan utilization as a carbon source for growth. Polymeric xylan and xylan-derivative use by *C. crescentus* was investigated in this work. Growth, enzyme, metabolite, and gene expression analyses show possible membrane-bound enzymes for xylan deconstruction on the cell surface while enzymes for further deconstruction of xylan-derived oligosaccharides are concentrated in the periplasm. TonB-dependent transporter (TBDT) inhibition data suggest that TBDT may be involved in the transport of xylo-oligosaccharides across the outer membrane. Collectively, data suggest xylan binding onto the bacterial surface and deconstruction and the xylan fragment uptake across the outer membrane. A comprehensive model for xylan utilization by *C. crescentus* develops to show features of previously proposed gut and plant pathogenic bacterial models. This study further advances the molecular level understanding of xylan derived nutrient acquisition in environmental bacteria.

1 | INTRODUCTION

Most microbial polysaccharide degradation studies focus on depolymerization of cellulose with significant reports of xylan degradation [1-4]. Unlike cellulose, xylan presents challenges for microbial degradation due to its chemical and structural heterogeneity that requires bacterial species to evolve with complex xylan deconstructing enzymes and other protein partners (Figure 1). These molecular partners are primarily composed of glycoside hydrolases (GH) and complex carbohydrate-binding modules (CBM). In addition to GH and CBMs, bacterial species have evolved with carbon compound sensing and specific membrane transporter mechanisms [1, 2].

Caulobacter crescentus (CB15) is a gram-negative, oligotrophic, alpha proteobacterium found in soil, freshwater lakes, streams, and marine environments. Many adaptations of *C. crescentus*, such as slow growth or complete arrest of cell cycle, presence of sessile and motile progenies, and enhanced nutrient uptake by the stalk of the sessile cells, help it survive in challenging nutrient-depleted or complex nutrient conditions [5, 6]. A characteristic feature of the carbohydrate utilizing system in many gram-negative bacteria, like *C. crescentus,* is the presence of Polysaccharide Utilization Loci (PUL). PUL is an organized cluster of genes, sometimes as operons, that codes for all the proteins required for the breakdown of a complex polysaccharide in a coordinated manner. Some of the proteins found in these complex molecular systems involve GH, CBMs, TonB-dependent transporters (TBDTs), carbohydrate sensors and transcriptional regulators [7].

The first PUL system uncovered was the Starch Utilization System, or Sus, in the human gut *Bacteroidetes* [8]. The Sus system has eight genes as a cluster, all of which encode for proteins on the outer-membrane that recognize starch and initiate hydrolysis, hydrolytic-intermediate transporters, and endo-glycosyl hydrolases, as well as transcriptional regulators [9, 10]. Of these

genes, there are two sequential genes; *susC* and *susD* that encode for an outer membrane TBDT and a cell-surface glycan-binding protein (SGBP) respectively [2]. This discovery serves as the model to describe other PUL systems from other bacteria, such as *Bacteroidetes and Xanthomonas spp*, found in diverse environments with common and unique features. For example, *Prevotella bryantii* in cow rumen [3] and the plant pathogen *Xanthomonas campestris* pv *campestris* [1] have evolved with complex xylan utilization systems.

Other gram-negative bacteria, including *C. crescentus,* also codes for similar clusters of genes. These clusters are slightly different than the Sus cluster with the absence of a few genes, such as a homolog for *susD gene,* but nevertheless serves to efficiently utilize complex carbohydrates [11]. Bacterial species have evolved to contain modified gene clusters to handle the wide range of complexity observed in polysaccharides, as shown in the case of the bacteria *B. ovatus,* which has two xylan-targeting PULs named XylS and XylL. These two clusters house different enzymes that could be used to break down β-xylans from distinct plant sources with unique structure [12]. Again, despite the modified enzymes for a specific substrate, the protein products of each PUL are still composed of proteins with clearly defined and similar functions, even if they might have distinct amino acid sequences [4].

While xylan-degrading genes in cow rumen bacteria were all found clustered in one locus, the plant pathogen bacteria *Xanthomonas campestris* has four loci of genes involved in the breakdown of xylan [1]. Such a plant pathogen also lacks an outer membrane xylanase and it has been suggested that *X. campestris* secretes xylanase into the carbohydrate rich environment. With such differences in the mode of xylan degradation among these bacterial species from unique nutritional niches, it is intriguing to probe a polysaccharide utilization system in an environmental bacterium that is capable of inhabiting a low-nutrient environment for comparative analysis of

xylan utilization mechanisms. The oligotrophic bacterium *C. crescentus* serves as an ideal model to learn about xylan utilization systems and mechanisms found in environmental bacteria.

2 | MATERIALS AND METHODS

2.1 | Culture conditions

C. crescentus (CB15) cells were grown in 250 mL of M2 minimal salt media supplemented with 0.2% (w/v) xylan (beech wood, Sigma-Aldrich, St. Louis, MO) as described previously [13, 14]. Culture media were inoculated with a frozen DMSO stock of CB15 cells and shaken at 30 ºC, 270 rpm. Two positive control cultures were established: one in xylose and the other one in glucose in M2 minimal medium. A negative control culture was established without any carbon source under the same experimental conditions. Xylan culture growth was monitored for growth by measuring optical density and colony forming unit counting at 600 nm (OD_{600}) for 8 days.

C. crescentus in xylo-oligosaccharide were cultured in a similar manner as described above. Briefly, 1 ml culture of 0.1% (W/V) minimal culture of the following carbon sources: 2^2-(4-*O*-Methyl-α-D-Glucuronyl)-xylotriose (OX3), 3^3-α-L-Arabinofuranosyl-xylotetraose (AX4), xylotetraose (X4) and xylopentaose (X5) (Megazyme), were prepared. Each culture was inoculated with a single colony of *C. crescentus* that has been grown on a PYE agar plate overnight at 37 ºC. and the culture growth was monitored by measuring the OD at 600.

2.2 | High performance liquid chromatography (HPLC) analysis

Carbohydrate composition of the cell-free (removed by centrifugation) growth media was filtered and analyzed by HPLC coupled with ELSD. Briefly, the media containing cells were spun at 9600x ***g*** rpm for 10 min to separate cells and then the supernatants were immediately placed in boiling water to inactivate any enzyme activity for five minutes. The media was then filtered with

a 0.22 µm filter attached to a syringe and ran through an Aminex 42C-HPX column maintained at 75 ºC oven. HPLC grade water was used as solvent and the flow rate was kept at 0.35 ml per minute for 40 minutes.

2.3 | Subcellular fractionation

C. crescentus xylan minimal media cultures collected at 0, 1, 2, 3, 4, and 5 days of growth from three biological replicates and cell pellets were collected by centrifugation at 9600x ***g*** for 10 min. Outer membrane fraction isolation published previously was followed with suitable modifications [11, 15]. Cells were then rinsed in a resuspension buffer of 50 mM Tris-HCl, pH 8.0 and centrifuged at 9600x ***g*** for 10 min to collect a pellet and re-suspended in 15 ml 60 mM Tris-HCl, 0.2 mM EDTA, pH 8.0. To the suspension, 0.5 ml of 4x protease inhibitor cocktail (PIC) (Thermo Scientific) and 150 µl of 1 mM PMSF in ethanol were added to inhibit any proteolytic degradation of enzymes [15]. Cells were sonicated at 10 watts in five cycles of 1 minute of sonication and 30 seconds of ice-cooling. The cell debris was pelleted at 9600x ***g*** for 25 min and to the supernatant that contains membrane fragments, 10 mL of extraction buffer consisting of 50 mM Tris-HCl, 10 mM $MgCl_2$, and 2% triton X-100 was added and mixed briefly. The mixture was centrifuged for 60 min at 38,000x ***g***. The resulting pellet which contains outer-membrane protein fraction was washed twice with 10 mL of sterile ice-cold water by transferring the water along the tube wall but not squirting directly into the pellet. The pellet which contains the outer membrane portion was resuspended in 0.5 mL of 10 mM Tris-HCl buffer at pH 7.0 and kept at 4 °C for subsequent enzymatic reactions.

Periplasmic protein isolation procedure was carried out as per the previously described protocol [15]. *C. crescentus* xylan minimal media cultures collected at 0, 1, 2, 3, 4, and 5 days of

growth from three biological replicates and cell pellets were collected by centrifugation at 9600x ***g*** for 10 min. The resulting pellet was resuspended in 5 mL of 10 mM Tris-Cl at pH 8.5 and the mixture was centrifuged at 9600x ***g*** for 10 min and the supernatant was discarded. The cell pellet was resuspended in 1 mL of 10 mM Tris-Cl buffer at pH 8.5 and treated with PIC and PMSF as stated above. To this mixture, 500 µL chloroform was added and vortexed briefly to mix. The reaction was left to incubate at room temperature for about 15 min. Then, 1 mL of 10 mM Tris-Cl buffer at pH 8.5 was added and mixed with the supernatant before centrifuged at 16,000x *g* for 20 min. The aqueous supernatant layer on top which contains Tris-Cl buffer and periplasmic proteins was collected and kept in 4 °C for subsequent enzymatic reactions. Periplasmic contents were tested for the cytoplasmic marker glucose-6-phosphate dehydrogenase to affirm absence of contamination as previously described [15].

Whole cell lysate protein isolation procedure was carried out as per the previously described protocol [15]. *C. crescentus* xylan minimal media cultures collected at 0, 1, 2, 3, 4, and 5 days of growth from three biological replicates and cell pellets were collected by centrifugation at 9600x ***g*** for 10 min. The resulting pellet was resuspended in 50 mM Tris-HCl buffer at pH 8.0 and washed twice before final resuspension in 1 ml of 10 mM Tris-HCl buffer at pH 8.0 and treated with PIC and PSMF. Cells were sonicated at 10 watts in cycles of 1 minute of sonication and 30 seconds of ice-cooling, repeated for a total of 5 times. The product was centrifuged briefly for 1 minute at 10,000x *g*, then the clear supernatant was transferred to individual Eppendorf tubes and kept in 4 °C for subsequent enzymatic reactions.

Three 50 ml of cell-free media were collected at select growth time points and treated with 0.5 mL protease inhibitor cocktail (Sigma-Aldrich). The samples were concentrated to roughly 3

mL using Amicon ultrafiltration cells fitted with 5000 kDa molecular mass cut-off filters at 4 °C under nitrogen gas.

2.4 | Enzyme assays

To measure the xylosidase activity of the subcellular fractions 20 µL of the fractions were incubated in a tube containing 250 µL of the 5mM *p*-nitrophenyl-β-D-xylopyranoside (*pNPX*) in 730 µL acetate buffer (pH 5.5) for 5 min at 37 °C. The reaction in each test tube was stopped by adding 1 ml of 0.2 M sodium hydroxide solution and the absorbance was measured immediately. To calculate the specific activity, protein quantification was carried out using Bradford assay following the manufacturer's instructions and previously published methods [15]. A unit of xylosidase activity was defined as the amount of enzyme necessary to release 1 µmol *p*-nitrophenol per minute.

In order to analyze the different types of enzyme activities present in the subcellular fractions, 20 µL of 0.2% (w/v) solutions of the following XOS substrates (OX3, AX3, X4, and X5) in 50 mM phosphate buffer pH 7.0 were incubated with the fractions at 37 °C in a water bath. After 12 h of incubation the products of the reaction were resolved by Thin Layer Chromatography (TLC) on Silica Gel HLF 250 µm (Analtech) plate using 85:15 (v/v) acetonitrile to water as the mobile phase. TLC plates were sprayed with freshly prepared 16 mM orcinol in 70% sulfuric acid. The plates were immediately placed in an oven at 70 °C for 15 min to visualize spots [16].

2.5 | Reverse transcription PCR (RT-PCR)

RNA isolation was carried out using TRIzol reagent and the bacterial RNA isolation protocol provided by the manufacturer (ThermoFisher). *C. crescentus* cell pellets were collected from 15 mL glucose and xylose growth cultures after 6 h of growth and from xylan growth culture after 2 days of growth and cell count was optimized prior to RNA isolation. RNA pellets obtained were resuspended in 30 µL of RNase-free water with 0.1 mM EDTA (Sigma). The samples were incubated in a 55 °C water bath for 10 min before subsequent reactions. Each RNA sample was tested for DNA contamination by running PCRs using B27F and U1492 *E. coli*. Reverse transcriptase polymerase chain reaction was carried out following the manufacturer's instructions using random hexamer primer (Promega). The cDNA products were kept at 4 °C for subsequent amplification reactions. Gene specific PCR was carried out using primers for the genes listed in Table 3 using standard PCR protocol provided by the manufacturer (Promega) and primer specific annealing temperature. PCR products were separated by 2% and visualized by ethidium bromide staining.

3 | RESULTS

3.1 | Xylan and xylo-oligosaccharides in minimal media support *C. crescentus* growth

M2 minimal media CB15 cultures were raised under standard sterile conditions as previously described with xylan or xylo-oligosaccharides (XOS) as a carbon source to investigate the ability of CB15 to utilize polymeric xylan as a carbon source [15]. CB15 growth in xylan or XOS were optically monitored with control cultures as shown in Figure 2. Additionally, colony forming unit technique was used in complement with OD_{600} measurements to further confirm the growth of *C. crescentus* in xylan minimal culture (data not shown). CB15 growth in xylan showed the characteristics of bacterial growth phases. The lag phase lasted for 3 days and was significantly

218 longer than the lag phase of 6 h observed in glucose, but interestingly, glucose, xylose and xylan
219 showed approximate log phases of 24 h. The highest OD_{600} value observed in xylan was relatively
220 lower than the maximum OD_{600} measurement recorded for growth in glucose but nearly four times
221 higher than the OD_{600} value recorded for xylose, suggesting the presence of growth promoting
222 xylan-derived carbon compounds in xylan cultures.

223 To further understand the nature of xylan utilization by *C. crescentus*, growth in
224 structurally different XOS (Figure 3) cultures in M2 minimal media were monitored as described
225 above. The growth curves in 2^2-(4-*O*-methyl-α-D-glucuronyl)-xylotriose (OX3), 3^3-α-L-
226 arabinofuranosyl-xylotetraose (AX4), xylotetraose (X4) and xylopentaose (X5) shown in Figure 4
227 display characteristic features of typical bacterial growth confirming that *C. crescentus* can utilize
228 all four XOS as the carbon source for growth. However, growth in each of the XOS displays
229 characteristic features, such as longest lager phase displayed by OX3 compared to much shorter
230 lag phases in other three xylo-oligosaccharide substrates (Table 1). Additionally, the two
231 xylotetraose cultures showed higher OD_{600} measurement than the OX3 or xylopentaose cultures,
232 suggesting growth dependence on the chemical structure and composition of the XOS.
233

234 **3.2 | Xylan degradation and degradation product uptake are coupled processes**

235 To study the xylanolytic process in CB15 growth cultures, extracellular growth media fractions
236 were collected over a period of 8 days and analyzed by HPLC along with standards of xylan,
237 xylose, arabinose, glucuronic acid and XOS. The xylan carbon source remained intact during the
238 sterilization (by autoclave) process as confirmed by HPLC and TLC analysis and the pH of the
239 xylan solution remained neutral before and after autoclaving [17, 18]. The chromatograms in
240 Figure 5 show the xylan peak at 9.7 min for all samples collected at different growth time points.

The two additional peaks appearing at retention times 11.3 min and 13.8 min stem from the M2 salt components as confirmed by minimal media analysis (data not shown). The xylan peak shows a significant decrease to more than half by the fifth day, and only about 5.5% of the xylan remained by the eighth day. The xylan reduction in the extracellular media parallels the growth trend observed in xylan carbon source (Figure 2). A significant decrease in xylan content observed after day three coincides with the end of the lag phase and the beginning of the log phase of growth.

To understand the xylan-derived carbon compound uptake, we investigated any roles played by TBDT using carbonyl cyanide 3-chlorophenylhydrazone (CCCP) [19] and the TBDT inhibitory TonB pentapeptide (Glu-Thr-Val-Ile-Val) [20] to potentially block the functions of TBDTs in *C. crescentus* grown in xylan, xylose and the xylo-oligosaccharide substrates. The effects of these TBDT interfering compounds toward *C. crescentus* growth is shown in Figure 6. In the presence of CCCP, *C. crescentus* growth in all six carbon sources show extension in the lag and log phases of CB15 growth as previously observed in the growth of *E.coli* in the presence of CCCP [19]. For xylose, this effect delays the log phase from 6 h to 24 h and the log phase takes 75 h to reach the maximum OD_{600} measurement when compared to the culture without CCCP (Figure 6A) and for xylan, the lag phase was extended for another 25 h compared to the culture without CCCP (Figure 6B). For both AX4 and X4, the lag phase was approximately 50 h (Figure 6D and 6E). For X5, the delay was a significant 94 h (Figure 6F). Surprisingly, OX3 experienced the most prolonged lag phase of 170 h in the presence of CCCP and only started to show slight increase on OD thereafter. Growth in X4 and X5 did not reach the maximum OD_{600} at the stationary phase observed for the culture without CCCP as seen in other cultures except in OX3. Interestingly, there was growth in TonB peptide, instead of growth arrest or delay as expected in all six cultures and reached a similar OD_{600} maximum as in control cultures. To explore this

observation, we raised a CB15 culture with TonB pentapeptide as the sole carbon source in minimal media and found that TonB pentapeptide supports growth of CB15 under these growth conditions (data not shown).

3.3 | The outer membrane and the periplasm contain xylan deconstructing enzymes

Xylanase specific activity in the extracellular media and the cellular fractions towards pNPX substrate were calculated and reported in U/mg of protein, in which one unit of activity is defined as the amount of enzyme that catalyzes the conversion of 1 μmol of *p*-nitrophenol per minute. Three independent isolates of enzyme fractions were used in each of the duplicate assays, and the mean value are shown in Figure 7. While the overall xylanase activity generally increased for all three cellular fractions up to three days and levels off, no measurable activity was detected for the extracellular media fraction at any growth time point tested. This suggests that no xylosidases are released into the extracellular media that are active towards *p*NPX substrate. Among the subcellular fractions, the highest specific activity of 919 U/mg was recorded for the periplasmic fraction isolated on day three of growth. Among the outer membrane fractions the highest specific activity of 67 U/mg was in the fractions collected on the fourth day of growth, and overall, the xylanase activity in outer membrane fractions can be considered constant within the margin of error from day 1 to day 5 of growth. The high specific activity observed in the periplasmic fractions were consistent from day 2 until 5 and this relatively high value compared to the outer membrane and the whole cell lysate suggest a high concentration of xylanase in the periplasmic space.

To gain further insight into the nature of xylan deconstruction we profiled the substrate specificity of the xylan deconstructing enzymes found in the subcellular fractions and the extracellular media XOS substrates and TLC. Figure 8 and Table 2 show the breakdown products

determined by the R_f values in comparison with standards after the treatment of the four substrates with the total enzyme isolated as growth progressed. Treatment of OX3 substrate with the whole-cell lysate fractions and the periplasmic fractions collected on day 4 and 7 produced spots that matched xylose and 4-*O*-methyl-α-D-glucuronic acid (MeGlcA) (Figure 8A). No product was detected from the reaction with whole-cell lysate and periplasmic fractions collected on day 1. The day 1 and 4 outer membrane fractions did not break down the substrate but two products were observed with the day 7 outer membrane fraction that matched the R_f values of MeGlcA and xylotriose suggesting appearance of glucuronidase activity very late in the growth on the membrane without xylosidase activity. No product was observed for the reaction between the extracellular media fraction and the substrate. Overall, TLC data suggest the presence of glucuronidase and xylosidase activity in the periplasm of *C. crescentus* and glucuronidase activity during the later phase of growth on the membrane.

Results from the reactions of fractions towards the AX4 substrate are shown in Figure 8B. Only the enzyme fractions from day 4 and 7 of the whole-cell lysate and periplasm produced breakdown products from AX4 substrate. R_f value of these spots (0.73) closely matches that of both xylose (R_f = 0.77) and arabinose (R_f = 0.75) (Table 2). Interestingly, the whole-cell lysate fraction from day 7 hydrolyzes the substrate completely and displays only one spot that must be composed of both xylose and arabinose, as evidenced by R_f values. This observation suggests that both xylosidase and arabinosidase activities must be present in the whole cell lysate for complete breakdown of the AX4 substrate. Although the day 7 whole-cell lysate fraction shows complete breakdown of the substrate under the reaction condition, the day 7 periplasmic fraction only shows partial hydrolysis as the original substrate is still prominently visible on the TLC plate. The extracellular media as well as the outer membrane fraction show no activity toward AX4. Overall,

the results show the presence of xylosidase and arabinosidase in protein extracted from the whole-cells of *C. crescentus*. The difference between the whole cell and the periplasm results and the lack of activity in the membrane fraction suggests that the arabinosidase that is active towards the AX4 substrate must be concentrated in the cytoplasm.

Figure 8C and 8D show the results from reactions between the fractions and the xylotetraose and xylopentaose substrates. Whole-cell lysate and periplasmic protein fractions from day 4 and 7 show complete breakdown of both substrates into monomer xylose under the reaction conditions. This shows that xylosidase enzymes in the periplasm can completely break down short-chain XOS into monomer xylose. Although the outer membrane fraction collected on the day 7 showed some level of activity towards *p*-nitrophenyl-β-D-xylopyranoside as shown in Figure 7, the outer membrane fraction surprisingly shows no product formation in the reaction with these xylo-oligosaccharide substrates. No enzyme activity was detected in the extracellular media at any growth time point. Overall, the enzyme activity analyses indicate the presence of xylosidase, arabinosidase and glucuronidase activities in specific subcellular fractions of *C. crescentus* grown in xylan minimal culture.

3.4 | *C. crescentus* expresses all required enzyme genes for complete xylan deconstruction

All potential *C. crescentus* genes coding for enzymes that may play a role in xylan deconstruction based on the conserved domain search predictions are listed in Table 3 and their expression in response to xylose and xylan carbon sources were tested. Total RNA was collected at mid-log phase of growth and reverse transcribed into cDNA and amplified using gene specific primers and shown in Figure 9. The endo xylanases CC_2802 and CC_3042 showed expression in both xylose and xylan carbon sources as well as all β-xylosidases, except CC_0989 which expressed only in

xylan, expressed in both xylose and xylan. We did not detect expression of the β-xylosidase CC_2357 in either of the carbon sources. The expression of α-L-arabinofuranosidase CC_1422, α-glucuronidase CC_2811 and the esterase CC_0771 genes have all been detected in both xylose and xylan carbon sources.

4 | DISCUSSION

The ability of *C. crescentus* to survive in low-nutrient environments suggests the presence of metabolic pathways and mechanisms allowing *C. crescentus* to use low-abundance carbohydrate-derived carbon sources as revealed by Carbohydrate-Active-Enzymes (http://www.cazy.org) [21]. Studies have shown that *C. crescentus* can utilize mono-, di- and oligosaccharides as carbon source for growth but polysaccharide utilization has not been widely reported [11, 15, 22, 23]. Here, we show evidence for the breakdown of the polymeric xylan into smaller fragments in a cell surface-bound manner before uptake of these fragments across the outer membrane of *C. crescentus* without releasing any fragments into the environment.

The prolonged lag phase observed in xylan suggest production of all the enzymes necessary for xylan utilization (TABLE 3) as previously observed in a *E. coli* promoter activity study using fluorescence reporters under nutrient limited conditions [24]. Lag phase allow the bacterial cells to achieve a higher cell division and maximum growth rates once cells transition to log phase. At the same time, the genes responsible for ribosome or amino acid biosynthesis are not actively expressed during lag phase and only once cells reach this checkpoint, the second phase of synthesis of amino acids ramps up to allow cells to grow bigger. Presence of a self-checkpoint mechanism especially makes sense for bacteria living in a nutrient-poor oligotrophic environment like *C. crescentus*. Boutte et al. identified a guanosine tetraphosphate (ppGpp)-mediated stringent

response mechanism in the experimental strain CB15N of *C. crescentus* under starvation [25]. Further studies of how stringent response mechanisms operate in CB15 in a xylan-only carbon source growth conditions may shed light on gene regulation and on other bacterial oligotrophic mechanisms.

The data suggest, as expected, that the chemical nature of the available carbon source influence bacterial lag phase. For example, the growth in OX3 substrate resulted in a much longer lag phase than the unsubstituted but longer X4 and X5 or the differently substituted AX3 XOSes as different enzymes require specific substrate requirements (Figure 3 and 4) [26, 27]. This may explain the longer OX3 lag phase as the α-glucuronidases have a deep active site pocket and require the *O*-2 position substituted xylose at the non-reducing end as opposed to the substituted middle xylose in OX3 (Figure 3) [28]. This suggests that α-glucuronidase activity may depend on a prior xylosidase activity to generate the suitable substrate from OX3 for α-glucuronidase to further fragment the carbon source.

Both the outer membrane and the periplasmic fractions show enzyme activity toward the *p*NPX substrate. *p*NPX is a very sensitive, nonspecific colorimetric substrate for β-xylosidases that cleave xylose from non-reducing ends of XOSes, whereas xylanases typically cleave internal β(1 → 4) xylosidic bonds thus enzymes belonging to both β-xylosidase or xylanase can release the *p*-nitrophenol resulting in the color change that is typically reported as xylosidase/xylanase activity. The outer membrane fraction only showed relatively low level of specific activity towards *p*NPX substrate, while the activity towards the four different xylo-oligosaccharide substrates were not detected, except towards the OX3 substrate on day 7 of growth (Figure 8A-D). This might suggest that xylanase(s) is (are) found tethered to the outer membrane of the bacteria and might need the association of the other proteins, such as a CBM in the PULs system, to work properly.

382 The outer membrane protein isolation procedure may have disrupted these protein associations
383 necessary for endo-xylanase activities.

384 A high specific activity for *p*NPX substrate observed in the periplasm suggests presence of
385 xylosidase/xylanase in the periplasm. Subcellular protein location prediction by PSORTb
386 (https://www.psort.org/psortb/) and Gneg-mPLoc (http://www.csbio.sjtu.edu.cn/bioinf/Gneg-
387 multi/) suggest two possible glycoside hydrolases, CC_2802 and CC_3054 to be localized in the
388 periplasmic space and xylosidases CC_0989 and CC_0813 in the cytoplasm (Table 3) [29, 30].
389 This suggest potential breakdown of the short chain XOS that are transported into the periplasm
390 and the cytoplasm of CB15 and this transport would require the activities of membrane transporters
391 on both the outer and inner membrane to deliver the short chain XOS into these subcellular
392 locations. Unlike many gram-negative bacteria, *C. crescentus* lacks OmpF-type outer membrane
393 porins, which facilitates diffusion of hydrophilic substrates from the environment through the
394 water-filled pores [31]. However, *C. crescentus* encodes for unusually high number of TBDTs that
395 are found on the outer membrane, as well as a high number of ABC (ATP-Binding Cassette)
396 transporters on the inner membrane [32]. Some of these active transporters, TBDTs and ABC
397 transporters, must therefore also be induced and expressed as they may be involved in transporting
398 specific short chained XOS. Previous studies have shown expression of TBDTs in response to
399 gluco-oligosaccharides, maltose and sucrose [15, 21, 33] and xylose not as an inducer for the
400 expression of ABC transporter in *C. crescentus* [34]. We hypothesize that XOS with specific
401 substituents may serve as an inducer for ABC transporter, as it would indicate the presence of
402 xylan-derived fragments in the periplasm.

403 As the picture of xylan utilization in *C. crescentus* evolves, insight into protein export into
404 various subcellular locations, including the membranes, would assist in the understanding of

405 complete deconstruction of xylan. The protein sequences of all the xylan utilizing genes were
406 analyzed using two signal sequence identifier programs: SignalIP
407 (http://www.cbs.dtu.dk/services/SignalP/) and TatP (https://services.healthtech.dtu.dk/service.
408 php?TatP-1.0) [14, 35]. In general, bacterial protein translocation follows one of the two known
409 pathways: the Sec or Tat pathway. The Tat pathway translocate proteins that are already folded in
410 the cytoplasm and relies on proton motive force to do so [36]. The genes CC_1422 and CC_2811
411 encode for α-L-arabinofuranosidase and α-glucuronidase respectively and both were predicted to
412 be on the inner membrane as per Gneg-mPloc predictor. Both possess signal peptides, suggesting
413 that they may be translocated to other subcellular locations from the cytoplasm for their functions
414 (Table 3). Arabinosidase and glucuronidase activities observed towards AX4 and OX3 substrates
415 in the periplasm suggest their activities must be localized in the periplasm as periplasm-facing
416 membrane-bound enzymes. Both substrates were completely turned into monomeric products,
417 suggesting that substituents in XOS may be removed to generate unsubstituted xylose backbone
418 in the periplasm for further breakdown into xylose or transportation of the xylose chain into the
419 cytoplasm for further breakdown. The ABC transporters on the inner membrane are most likely
420 also involved in transportation of the xylan-derivatives into the cytoplasm in *C. crescentus* as
421 shown in malto-oligosaccharide transport by ABC transporters in *Streptococcus* [37].

422 The CC_2803 and CC_3042 are two GH 10 family endo-xylanases and both were
423 expressed in xylose and xylan carbon sources (Figure 9) and these enzymes may play crucial role
424 in the deconstruction of xylan by *C crescentus* as they cleave internal β-1,4-glycosidic linkages [2,
425 38]. Among the glycoside hydrolase families, GH 10 is the most extensively studied one [21]. GH
426 10 enzymes cleave the glycosidic linkage between substituted xylose monomers, like *O*-methyl
427 glucuronic acid or arabinose, and the xylose next to it [37, 39]. These structurally variable xylo-

oligosaccharide products may serve as substrates for different enzymes that further cleave off the substituents to generate plain xylo-oligosaccharide for efficient release of xylose. In general, the gene expression analysis suggests expression of most of the xylan deconstruction related genes in both xylose as well as xylan carbon sources, suggesting that xylose may function as an inducer for the expression of these genes.

The gene CC_3042 encodes for the conserved xylanase Xyn10C found among many xylan utilizing bacteria. In *Xanthomonas campestris* pv. *campestris*, a plant pathogen that causes black rot in cruciferous vegetables, Xyn10C is encoded by the gene XCC_4115, and is one of the three detected xylanases in *Xanthomonas campestris* pv. *campestris*' genome and contains signal peptide for secretion out of the cytoplasm [1]. A homolog of Xyn10C is also found in the XUS system (encoded as PBR_0377) of the human gut microbe *P. Bryantii*. This homolog has an *N*-terminal signal peptidase II cleavage site, which suggests that it is an outer membrane-anchored protein with a similar function as the SusG protein of *B. thetaiotaomicron*, an obligate anaerobe and an opportunistic pathogen found in human gut flora [3, 8, 9]. This homology feature reflects the presence of highly conserved carbohydrate utilization systems, in terms of protein sequence, three dimensional structures and enzymatic activity, across the microbial communities of different niches and nutrient acquisition modes and yet they also display variety [40].

The presence of Tat signal in CC_2803 implies this enzyme might as well be targeted for translocation to other subcellular locations (Table 3). This gene is also located in the vicinity of CC_2802, CC_2811 and CC_2804, which encode for a xylosidase and a α-glucuronidase and a TBDT respectively. Both CC_2802 and CC_2811 are expressed under xylose carbon source conditions, and in fact, D-xylose has been shown to induce the expression of over 50 genes in *C. crescentus* [14] [41, 42]

TonB pentapeptide did not cause growth retardation or arrest due to expected inhibition of TonB transport function as postulated in this study. However, CCCP incurred a significantly longer lag phase for xylan and all xylo-oligosaccharide substrates. This effect was not observed for CB15 xylose minimal media culture induced with CCCP, which might be due to the presence of OprB protein on the outer membrane of CB15 that allows diffusion of xylose into the cell across the outer membrane as OprB has been shown to transport wide range of hydrophilic molecules including different monosaccharides [15, 43]. Presence of CCCP in bacterial cultures has been shown to slow down the growth [44]. For larger substrate transportation, *C. crescentus* may rely heavily on TBDTs and impairment of proton motive force that is necessary for the function of TBDTs may have result in the longer lag phase as observed. TBDTs have been shown with more functions than just transportation of larger nutrient molecules across the outer membrane such extracytoplasmic function σ factor (ECF) mediated regulation of gene expression as observed in *B. thetaiotaomicron* [3, 8, 45].

The PUL system, in which a collective group of proteins with different functional roles work together to effectively breakdown xylan extracellularly into smaller fragments and uptake the breakdown products across cell membrane via transporters has been reported in bacteria that inhabit plants and animal gut [1, 3]. If this is the case for *C. crescentus* then a model for xylan utilization develops with an outer membrane-bound xylanase to break the xylan backbone on the cell surface into smaller fragments. This xylanase may work together with carbohydrate binding proteins or with a CBM and a transporter to capture and transport the cleaved xylo-oligosaccharides across the membrane into the periplasm without releasing into the environment. An amino acid sequence analysis of the membrane binding domains using TMHMM server identified CC_0813 and CC_3054 to contain an *N*-terminal sequence with high tendency to

function as a membrane tether. Additionally, we identified two TBDTs (CC_0185 and CC_1666) and another outer membrane protein pump (OmpA, CC_3494) (unpublished data) in a comparative proteomic analysis of *C. crescentus* grown in xylose and xylan that may play a role in this function but further experiments are required to confirm the functional roles of these proteins. An alternative model of extracellular xylanase mediated breakdown of xylan is not supported by our data (Table 2) [1]. Furthermore, releasing fragmented XOS into an aquatic environment is not an economically viable mode of nutrient acquisition for an oligotrophic organism. A previous study from our lab on gluco-oligosaccharide utilization in M2 minimal media using gluco-oligosaccharides as the carbon source by *C. crescentus* showed breakdown products in the extracellular media [15]. The gluco-oligosaccharides used by Presley *et al.*, as opposed to polymeric xylan, extended only up to cellotetraose and it may not have bound to a CBM thus upon cleavage of glycosidic linkage it may be released into the environment as shown in that study [15].

Based on the observations made in this study and the collective and comparative analysis of the genomics related to xylan utilization in *C. crescentus* and related organisms, a predictive model of xylan utilization system in *C. crescentus* is proposed in Figure 10.

ACKNOWLEDGEMENTS

The authors would like to thank Jessica Derham for careful reading of the manuscript and Eastern Illinois University for funding. Authors thank Drs. Aretha Fiebig, Michigan State University and Sean Crosson, University of Chicago for bacterial strain and technical advice related to *Caulobacter crescentus* cultures.

CONFLICT OF INTERESTS

The authors have declared no conflict of interests.

DATA AVAILABILITY STATEMENT

The data that support the findings of this study are available from the corresponding author upon reasonable request.

References

[1] Déjean G, Blanvillain-Baufumé S, Boulanger A, Darrasse A, de Bernonville TD, Girard AL, et al. The xylan utilization system of the plant pathogen *Xanthomonas campestris pv campestris* controls epiphytic life and reveals common features with oligotrophic bacteria and animal gut symbionts. New Phytol. 2013;198:899-915.

[2] Déjean G, Tauzin AS, Bennett SW, Creagh AL, Brumer H. Adaptation of Syntenic Xyloglucan Utilization Loci of Human Gut *Bacteroidetes* to Polysaccharide Side Chain Diversity. Appl Environ Microbiol. 2019;85:e01491-19.

[3] Dodd D, Mackie RI, Cann IK. Xylan degradation, a metabolic property shared by rumen and human colonic Bacteroidetes. Mol Microbiol. 2011;79:292-304.

[4] Larsbrink J, Thompson AJ, Lundqvist M, Gardner JG, Davies GJ, Brumer H. A complex gene locus enables xyloglucan utilization in the model saprophyte *Cellvibrio japonicus*. Mol Microbiol. 2014;94:418-433.

[5] Ireland MM, Karty JA, Quardokus EM, Reilly JP, Brun YV. Proteomic analysis of the *Caulobacter crescentus* stalk indicates competence for nutrient uptake. Mol Microbiol. 2002;45:1029-1041.

[6] Laub MT, Shapiro L, McAdams HH. Systems biology of Caulobacter. Annu Rev Genet. 2007;41:429-441.

528 [7] Grondin JM, Tamura K, Déjean G, Abbott DW, Brumer H. Polysaccharide Utilization
529 Loci: Fueling Microbial Communities. *J Bacteriol*. 2017;199:e00860-16.
530
531 [8] Martens EC, Koropatkin NM, Smith TJ, Gordon JI. Complex glycan catabolism by the
532 human gut microbiota: the Bacteroidetes Sus-like paradigm. J Biol Chem.
533 2009;284:24673-24677.
534
535 [9] Reeves AR, D'Elia JN, Frias J, Salyers AA. A *Bacteroides thetaiotaomicron* outer
536 membrane protein that is essential for utilization of maltooligosaccharides and
537 starch. J Bacteriol. 1996;178:823-830.
538
539 [10] Cho KH, Cho D, Wang GR, Salyers AA. New regulatory gene that contributes to
540 control of *Bacteroides thetaiotaomicron* starch utilization genes. J Bacteriol.
541 2001;183:7198-7205.
542
543 [11] Neugebauer H, Herrmann C, Kammer W, Schwarz G, Nordheim A, Braun V. ExbBD-
544 dependent transport of maltodextrins through the novel MalA protein across the
545 outer membrane of *Caulobacter crescentus*. J Bacteriol. 2005;187:8300-8311.
546
547 [12] Rogowski A, Briggs JA, Mortimer JC, et al. Glycan complexity dictates microbial
548 resource allocation in the large intestine. Nat Commun. 2015;6:7481.
549
550 [13] Ely B. Genetics of *Caulobacter crescentus*. Methods Enzymol. 1991;204:372-384.

[14] Hottes AK, Meewan M, Yang D, Arana N, Romero P, McAdams HH, et al. Transcriptional profiling of *Caulobacter crescentus* during growth on complex and minimal media. J Bacteriol. 2004;186:1448-1461.

[15] Presley GN, Payea MJ, Hurst LR, Egan AE, Martin BS, Periyannan GR. Extracellular gluco-oligosaccharide degradation by *Caulobacter crescentus*. Microbiology (Reading). 2014;160:635-645.

[16] Hrmova M, Burton RA, Biely P, Lahnstein J, Fincher GB. Hydrolysis of (1,4)-beta-D-mannans in barley (*Hordeum vulgare L.*) is mediated by the concerted action of (1,4)-beta-D-mannan endohydrolase and beta-D-mannosidase. Biochem J. 2006;399:77-90.

[17] Joksimovic G, Markovic Z. Investigation of the Mechanism of Acidic Hydrolysis of Cellulose. Acta Agriculturae Serbica. 2007:12:51-57.

[18] Lohmiller S, Hantke K, Patzer SI, Braun V. TonB-dependent maltose transport by *Caulobacter crescentus*. Microbiology (Reading). 2008;154(Pt 6):1748-1754.

[19] Kinoshita N, Unemoto T, Kobayashi H. Proton motive force is not obligatory for growth of *Escherichia coli*. J Bacteriol. 1984;160:1074-1077.

[20] Tuckman M, Osburne MS. In vivo inhibition of TonB-dependent processes by a

574 TonB box consensus pentapeptide. J Bacteriol. 1992;174(1):320-323.
575
576 [21] Cantarel BL, Coutinho PM, Rancurel C, Bernard T, Lombard V, Henrissat B. The
577 Carbohydrate-Active EnZymes database (CAZy): an expert resource for
578 Glycogenomics. Nucleic Acids Res. 2009;37(Database issue):D233-D238.
579
580 [22] Blanvillain S, Meyer D, Boulanger A, Guynet C, Denancé N, Vasse J, et al. Plant
581 carbohydrate scavenging through tonB-dependent receptors: a feature shared by
582 phytopathogenic and aquatic bacteria. PLoS One. 2007;2:e224.
583
584 [23] Arellano BH, Ortiz JD, Manzano J, Chen JC. Identification of a dehydrogenase
585 required for lactose metabolism in *Caulobacter crescentus*. Appl Environ Microbiol.
586 2010;76:3004-3014.
587
588
589 [24] Madar D, Dekel E, Bren A, Zimmer A, Porat Z, Alon U. Promoter activity dynamics in
590 the lag phase of *Escherichia coli*. BMC Syst Biol. 2013;7:136-149.
591
592 [25] Boutte CC, Crosson S. The complex logic of stringent response regulation in
593 Caulobacter crescentus: starvation signalling in an oligotrophic environment. Mol
594 Microbiol. 2011;80(3):695-714.
595
596 [26] Blagodatskaya E, Blagodatsky S, Anderson TH, Kuzyakov Y. Microbial growth and

carbon use efficiency in the rhizosphere and root-free soil. PLoS One. 2014;9: e93282.

[27] Ho A, Di Lonardo DP, Bodelier PL. Revisiting life strategy concepts in environmental microbial ecology. FEMS Microbiol Ecol. 2017;93:1-14

[28] Nurizzo D, Nagy T, Gilbert HJ, Davies GJ. The structural basis for catalysis and specificity of the *Pseudomonas cellulosa* alpha-glucuronidase, GlcA67A. Structure. 2002;10:547-556.

[29] Yu NY, Wagner JR, Laird MR, Melli, G., Rey, S., Lo, R et al. PSORTb 3.0: improved protein subcellular localization prediction with refined localization subcategories and predictive capabilities for all prokaryotes. Bioinformatics. 2010;26:1608-1615.

[30] Shen HB, Chou KC. Gneg-mPLoc: a top-down strategy to enhance the quality of predicting subcellular localization of Gram-negative bacterial proteins. J Theor Biol. 2010;264:326-333.

[31] Nierman WC, Feldblyum TV, Laub MT, et al. Complete genome sequence of *Caulobacter crescentus. Proc Natl Acad Sci U S A*. 2001;98(7):4136-4141.

[32] Young J, Holland IB. ABC transporters: bacterial exporters-revisited five years on. *Biochim Biophys Acta*. 1999;1461(2):177-200.

[33] Rees DC, Johnson E, Lewinson O. ABC transporters: the power to change. *Nat Rev Mol Cell Biol*. 2009;10(3):218-227.

[34] Modrak SK, Melin ME, Bowers LM. SucA-dependent uptake of sucrose across the outer membrane of *Caulobacter crescentus*. *J Microbiol*. 2018;56(9):648-655.

[35] Almagro Armenteros JJ, Tsirigos KD, Sønderby CK, et al. SignalP 5.0 improves signal peptide predictions using deep neural networks. *Nat Biotechnol*. 2019;37(4):420-423.

[36] Bendtsen JD, Nielsen H, Widdick D, Palmer T, Brunak S. Prediction of twin-arginine signal peptides. *BMC Bioinformatics*. 2005;6:167.

[37] Webb AJ, Homer KA, Hosie AH. Two closely related ABC transporters in Streptococcus mutans are involved in disaccharide and/or oligosaccharide uptake. *J Bacteriol*. 2008;190(1):168-178.

[38] Dodd D, Cann IK. Enzymatic deconstruction of xylan for biofuel production. *Glob Change Biol Bioenergy*. 2009;1(1):2-17.

[39] Maslen SL, Goubet F, Adam A, Dupree P, Stephens E. Structure elucidation of arabinoxylan isomers by normal phase HPLC-MALDI-TOF/TOF-MS/MS. *Carbohydr Res*. 2007;342(5):724-735.

643 [40] Kolenová K, Vrsanská M, Biely P. Mode of action of endo-beta-1,4-xylanases of
644 families 10 and 11 on acidic xylooligosaccharides. *J Biotechnol*. 2006;121(3):338-345.
645
646 [41] Stephens C, Christen B, Watanabe K, Fuchs T, Jenal U. Regulation of D-xylose
647 metabolism in *Caulobacter crescentus* by a LacI-type repressor. *J Bacteriol*.
648 2007;189(24):8828-8834.
649
650 [42] Berlemont R, Martiny AC. Phylogenetic distribution of potential cellulases in
651 bacteria. *Appl Environ Microbiol*. 2013;79(5):1545-1554.
652
653 [43] Wylie JL, Worobec EA. The OprB porin plays a central role in carbohydrate uptake in
654 Pseudomonas aeruginosa. *J Bacteriol*. 1995;177(11):3021-3026.
655
656 [44] Nakano S, Onoda T. Effect of protonophore on growth of Escherichia coli. *J Basic*
657 *Microbiol*. 1989;29(3):163-169.
658
659 [45] Postle K, Kadner RJ. Touch and go: tying TonB to transport. *Mol Microbiol*. 2003;49(4):
660 869-882.
661
662
663
664
665

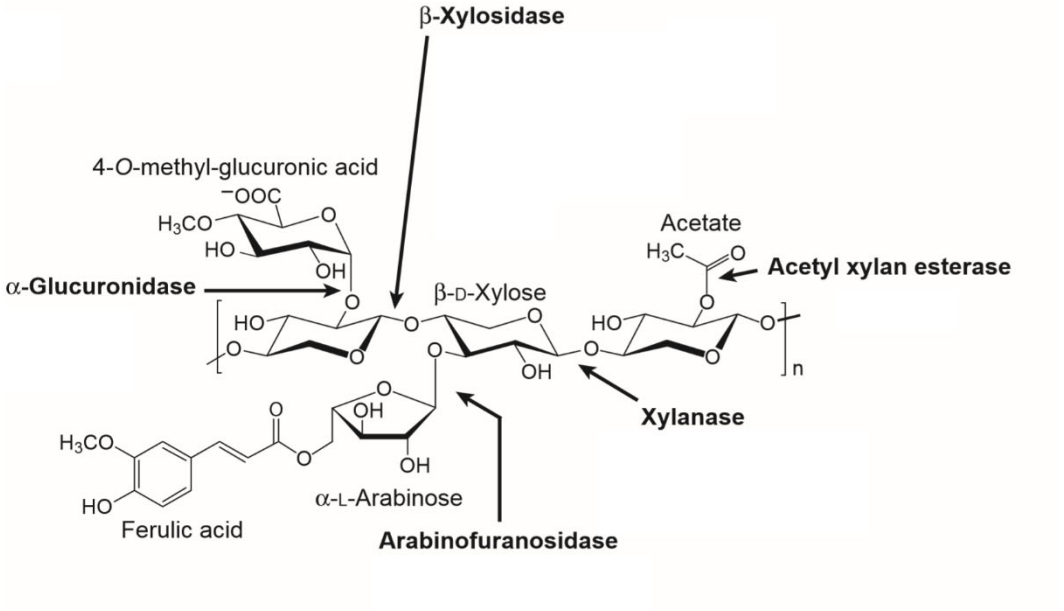

FIGURE 1 General chemical structure of xylan showing different linkages and associated enzyme activities.

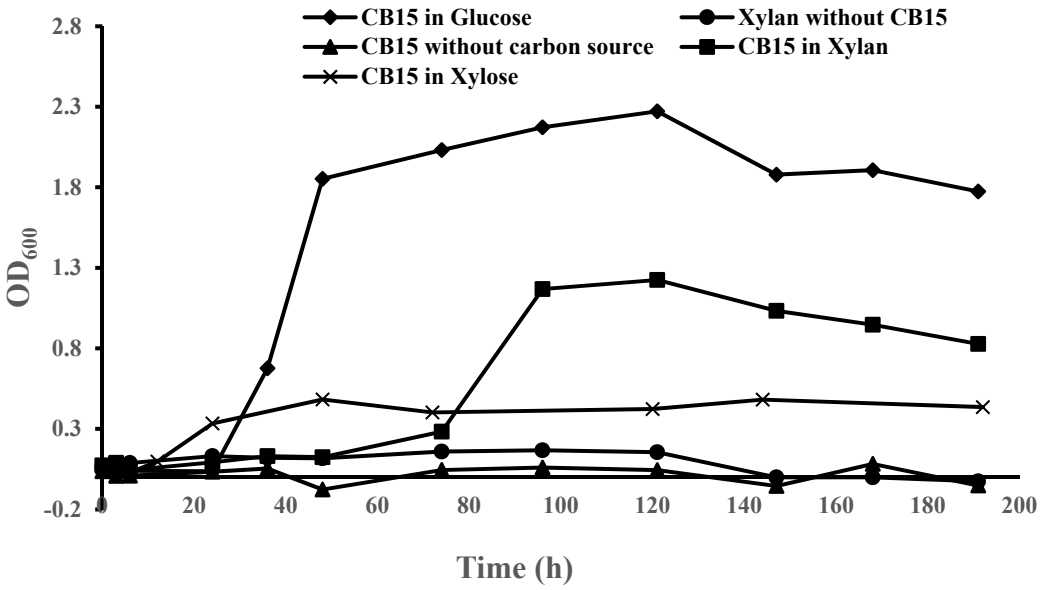

675
676 **FIGURE 2** *C. crescentus* growth in xylan. Growth time-dependent OD_{600} measurements of *C.*
677 *crescentus* cultures in M2 minimal media supplemented with 0.2% (w/v) of xylan or 0.2% (w/v)
678 glucose and control cultures and grown at 30 ºC, 260 rpm.
679
680
681

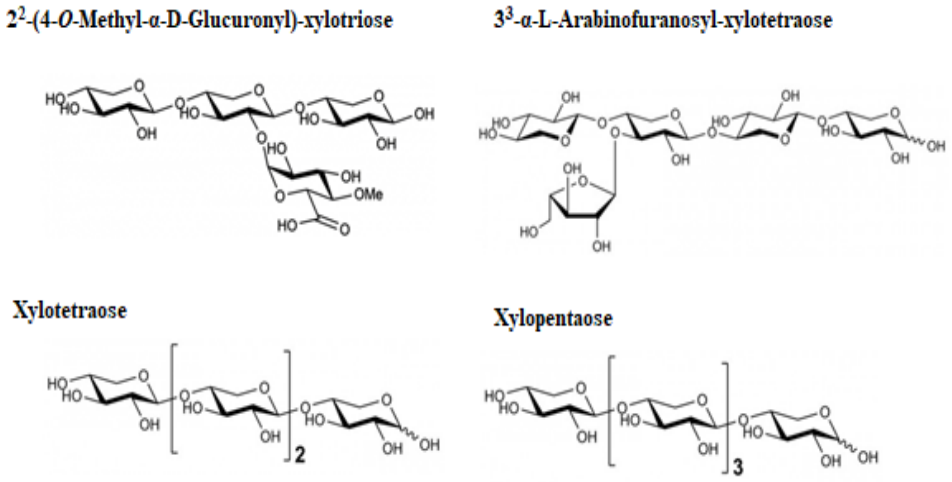

682
683 **FIGURE 3** Chemical structures of 2^2-(4-*O*-Methyl-α-D-Glucuronyl)-xylotriose (OX3),
684 3^3-α-L-Arabinofuranosyl-xylotetraose (AX4), xylotetraose (X4) and xylopentaose (X5).
685
686
687
688
689

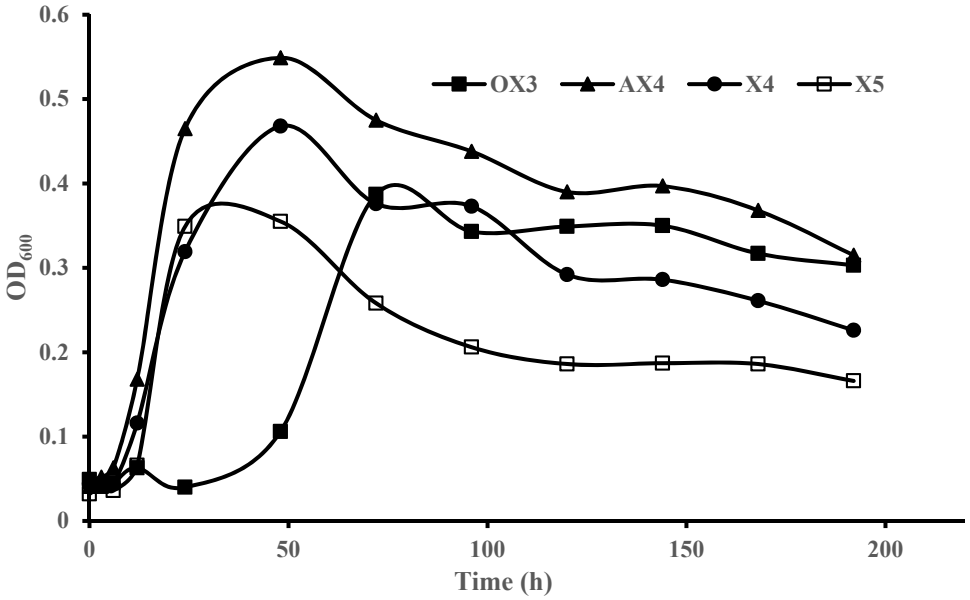

FIGURE 4 *C. crescentus* growth in XOS. Time-dependent OD_{600} of *C. crescentus* in M2 minimal media cultures supplemented with 0.1% (w/v) of 2^2-(4-*O*-Methyl-α-D-Glucuronyl)-xylotriose (OX3), 3^3-α-L-Arabinofuranosyl-xylotetraose (AX4), xylotetraose (X4) and xylopentaose (X5).

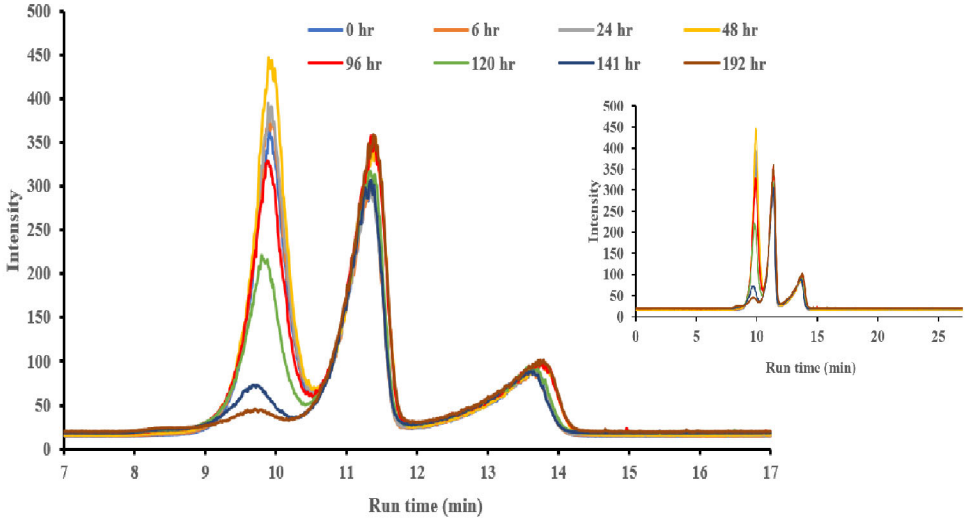

FIGURE 5 HPLC chromatogram of extracellular growth media of 0.2% (w/v) autoclaved xylan in M2 minimal salt. An Aminex HPX-42C column with water as mobile phase was used at 75 °C and compounds were detected with an ELSD detector using the same detection parameters as in standard compound detection. A full HPLC chromatogram of all the samples is shown in the inset.

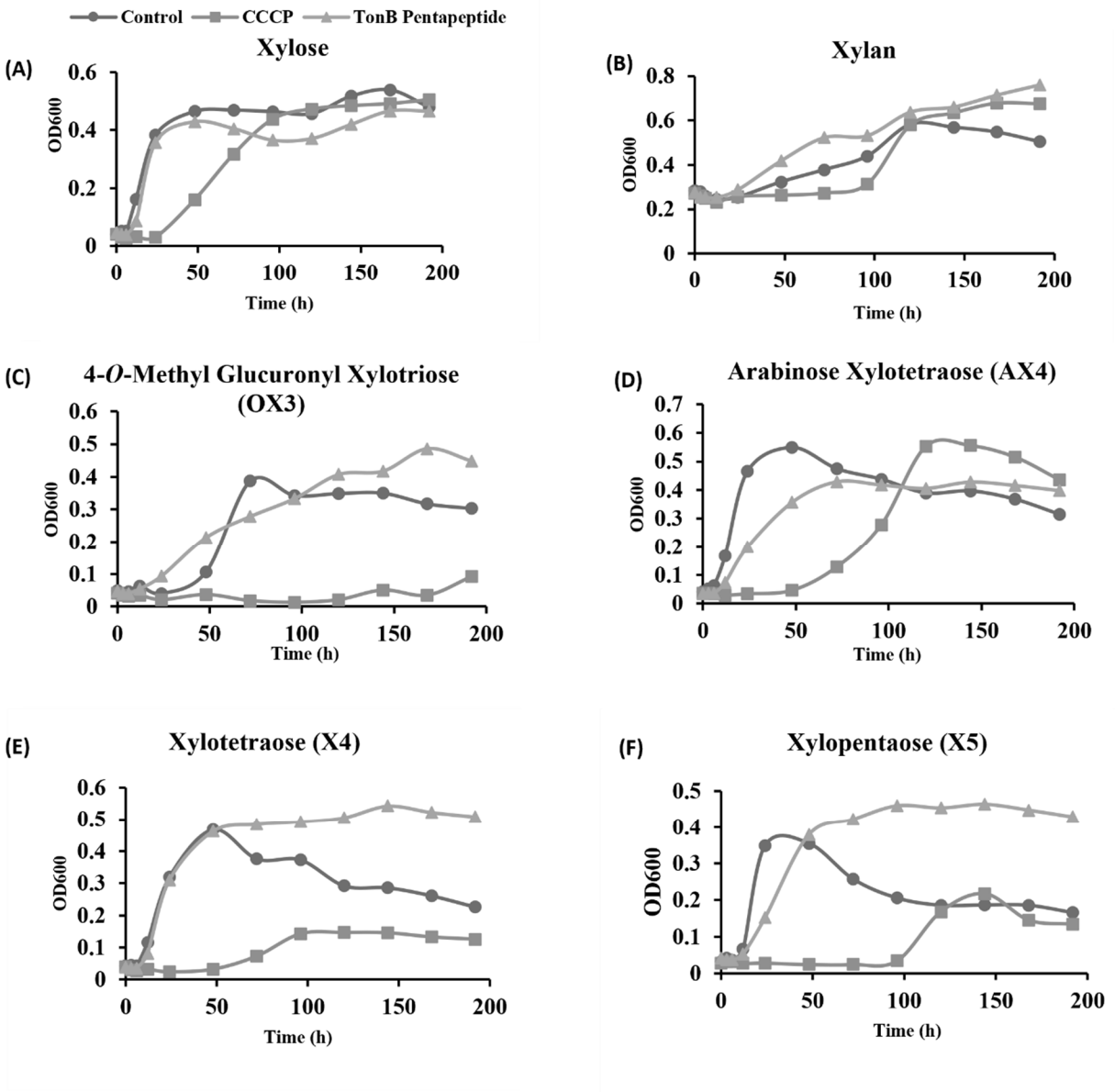

706
707 **FIGURE 6:** *C. crescentus* growth in minimal cultures containing one of the following: 0.2 %
708 (w/v) xylose, 0.2 % (w/v) xylan, 0.1 % (w/v) 4-*O*-methyl glucuronyl xylotriose, 0.1 % (w/v)
709 arabinose xylotetraose, 0.1 % (w/v) xylotetraose, 0.1 % (w/v) xylopentaose under the presence of
710 either: 10 µM CCCP or TonB pentapeptide at 100 µg/ml. All the cultures were monitored with
711 OD_{600} for 8 days.
712
713
714
715

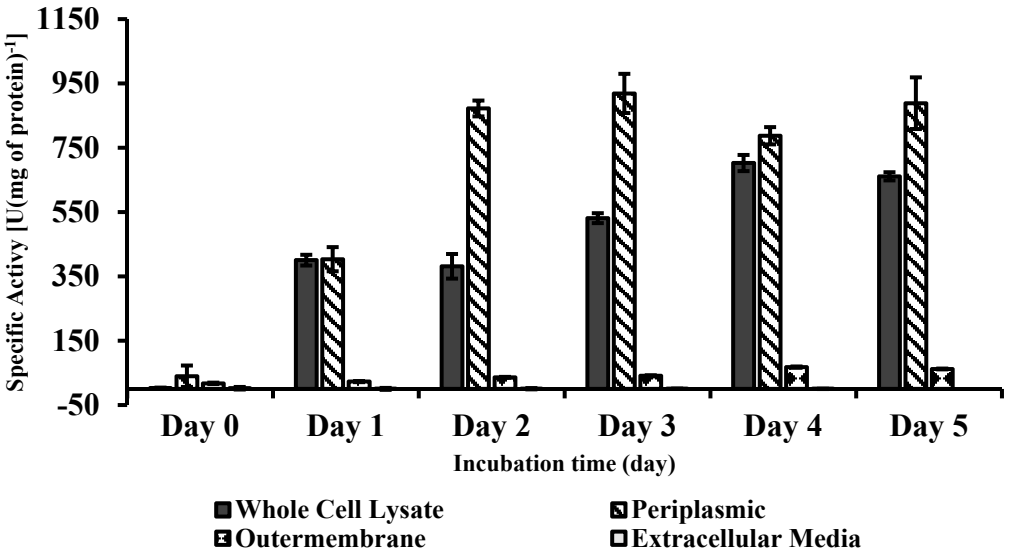

FIGURE 7 Xylanase activity of subcellular protein fractions and extracellular medium of xylan growth culture at 0, 1, 2, 3, 4 and 5 days of growth. Activities were calculated by measuring the *p*-nitrophenol released from *p*NPX substrate at 405 nm. All data points are the mean of duplicate assays of three independently isolated fractions.

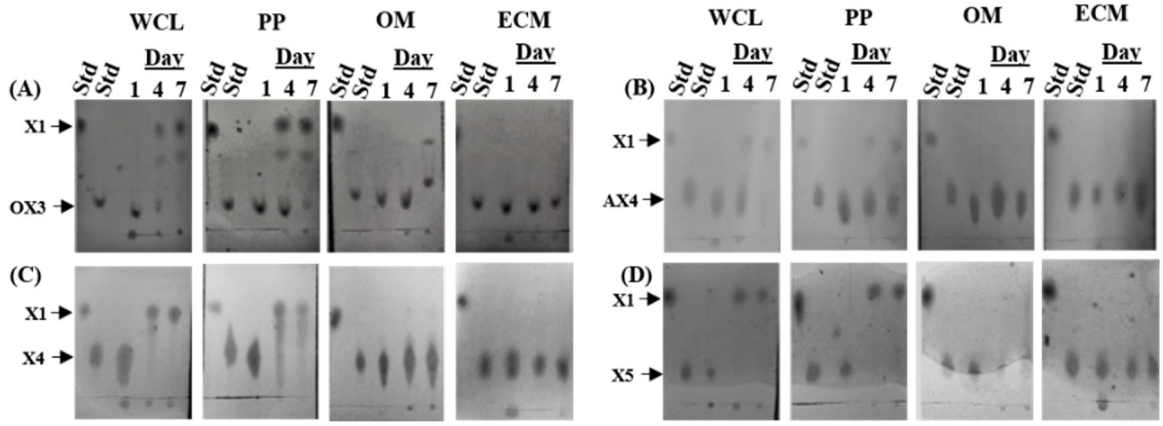

FIGURE 8 Thin layer chromatography analysis of the enzyme activities of subcellular protein fractions (WCL-Whole-cell lysate; PP-periplasm; OM-outer membrane) and extracellular medium (ECM) of xylan growth culture collected at day 1, 4, and 7 towards (A) 2^3-(4-*O*-methyl-α-D-glucuronyl)-xylotriose (OX3), (B) arabinofuranosyl-xylotetraose (AX4), (C) xylotetraose (X4) (D) xylopentaose (X5) substrates. Spots resolved on silica gel HLF 250 µm plates using 85:15 acetonitrile and water as solvent. The plate was sprayed with 16 mM orcinol in 70% sulfuric acid and developed in an oven at 90 °C for 10 min.

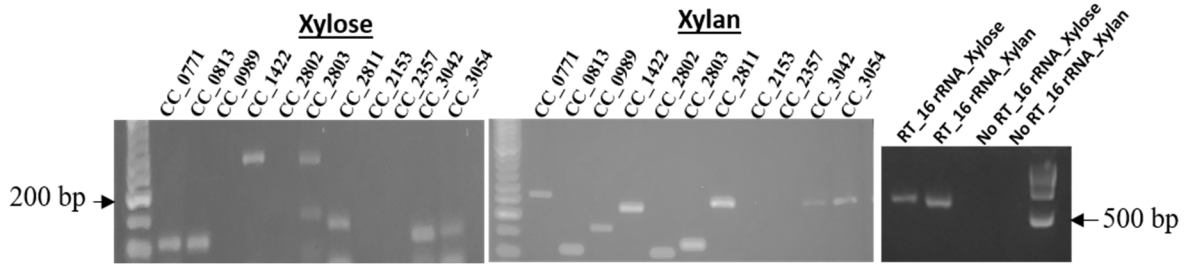

FIGURE 9 Reverse-Transcriptase (RT-PCR) based analyses for expression of *C. crescentus* genes in xylose (a) and xylan (b) carbon sources in minimal media cultures. rRNA control using 785F and 1492R (c). Gene locus tags (CC numbers) are shown above images. Expected amplicon size range from 40 to 180 bp except for the rRNA amplicon, which is around 700 bp.

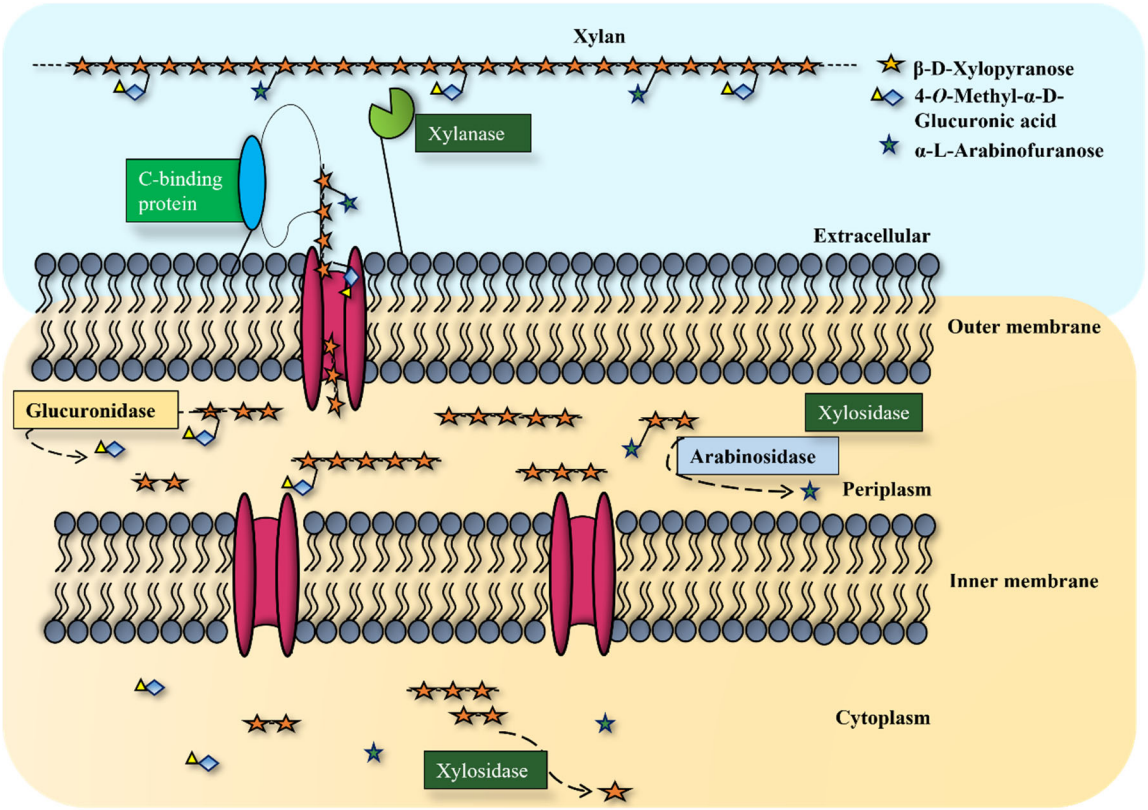

FIGURE 10 Proposed model for xylan degradation and uptake by *C. crescentus*. Endo-xylanases coded by CC_2803 and CC_3042 act as the extracellular xylanase that break down long chain xylan polymer into short XOS that could be substituted with arabinose, *O*-methyl glucuronic acid. These shorter chains are transported across the outer membrane by TonB-dependent receptor transporters. Short chain XOS are removed of substituents by α-glucuronidase (CC_2811) and arabinosidase (CC_1422) in the periplasm, and further degraded into xylose monomers either in the periplasm (with xylosidases encoded from CC_0813, CC_2802 and CC_3054) or cytoplasm (xylosidase CC_0989), then converted to D-xylonolactone by xylose dehydrogenase before further transformation into α-ketoglutarate, an intermediate of the citric acid cycle.

TABLE 1 Growth profile of *C. crescentus* in 2^2-(4-*O*-methyl-α-D-glucuronyl)-xylotriose (OX3), 3^3-α-L-arabinofuranosyl-xylotetraose (AX4), xylotetraose (X4) and xylopentaose (X5) carbon sources in M2 minimal media.

	OX3	**AX4**	**X4**	**X5**
Lag phase	24 h	6 h	6 h	12 h
Log phase	48 h	40 h	40 h	12 h
Max OD_{600}	0.387	0.549	0.468	0.355

TABLE 2 Summary of subcellular enzymatic activity of *C. crescentus* grown in xylan minimal culture towards 2^2-(4-*O*-methyl-α-D-glucuronyl)-xylotriose (OX3), 3^3-α-L-arabinofuranosyl-xylotetraose (AX4), xylotetraose (X4) and xylopentaose (X5).

	OX3	**AX4**	**X4**	**X5**	**Potential Enzyme Activity**
Whole Cell Lysate	Xylose MeGlcA	Xylose /Arabinose	Xylose	Xylose	Xylosidase, Arabinosidase, Glucuronidase
Periplasm	Xylose MeGlcA	Xylose /Arabinose	Xylose	Xylose	Xylosidase, Arabinosidase, Glucuronidase
Outer membrane	X3 MeGlcA	None	None	None	Glucuronidase
Extracellular Media	None	None	None	None	None

774 **TABLE 3** Xylan modifying enzymes in *C. crescentus.*

Putative Xylan Modifying Enzyme Activity/ Gene Code (GH Family)	Predicted Subcellular Location/s	Translocation Signal (Signal P /TatP)
Endo-β-1,4-xylanase (XYN)		
CC_2803 (GH10)	Periplasm/Inner membrane	Tat
CC_3042 (GH10)	Cytoplasm/Inner membrane	Tat
β-D-xylosidase (XYL)		
CC_0989 (GH43)	Multiple locations/Cytoplasm	None
CC_2357 (GH39)	Cytoplasm/Inner membrane	None
α-L-Arabinofurosidase (ARA)		
CC_1422 (GH51)	Cytoplasm/Inner membrane	Tat
XYN/XYL/ARA		
CC_0813 (GH43)	Multiple locations/Inner membrane	Tat
CC_2802 (GH43)	Multiple locations/Periplasm	None
CC_3054 (GH3)	Periplasm	Tat
α-Glucuronidase		
CC_2811(GH67)	Multiple locations/Inner membrane	None
Esterase		
CC_0771	Periplasm/Cytoplasm	None
Deacetylase		
CC_2153	Periplasm	Tat

775
776
777
778
779
780
781
782
783
784